RESEARCH ARTICLE

A novel bioactive PEEK/HA composite with controlled 3D interconnected HA network

Mohammad Vaezi and Shoufeng Yang*

Faculty of Engineering & the Environment, University of Southampton, SO17 1BJ, UK

Abstract: Polyetheretherketone (PEEK) is a high-performance thermoplastic biomaterial which is currently used in a variety of biomedical orthopaedic applications. It has comparable tensile and compressive strength to cortical bone with favourable biocompatibility. However, natural grade PEEK-OPTIMA has shown insufficient bioactivity and limited bone integration. Bioactive PEEK composites (e.g., PEEK/calcium phosphates or Bioglass) and porous PEEK have been used to improve bone-implant interface of PEEK-based devices, but the bioactive phase distribution or porosity control is poor. In this paper, a novel method is developed to fabricate a bioactive PEEK/hydroxyapatite (PEEK/HA) composite with a unique configuration in which the HA (bioactive phase) distribution is computer-controlled within a PEEK matrix. This novel process results in complete interconnectivity of the HA network within a composite material, representing a superior advantage over alternative forms of product. The technique combines extrusion freeforming, a type of additive manufacturing (AM), and compression moulding. Compression moulding parameters, including pressure, temperature, dwelling time, and loading method together with HA microstructure were optimized by experimentation for successful biocomposite production. PEEK/HA composites with a range of HA were produced using static pressure loading to minimise air entrapment within PEEK matrix. In addition, the technique can also be employed to produce porous PEEK structures with controlled pore size and distribution.

Keywords: polyetheretherketone (PEEK); additive manufacturing (AM); bioactive PEEK/HA composite

*Correspondence to: Shoufeng Yang, Faculty of Engineering & the Environment, University of Southampton, SO17 1BJ, UK; Email: s.yang@soton.ac.uk

Received: May 25, 2015; **Accepted:** June 17, 2015; **Published Online:** July 2, 2015

Citation: Vaezi M and Yang S F, 2015, A novel bioactive PEEK/HA composite with controlled 3D interconnected HA network. *International Journal of Bioprinting*, vol.1(1): 66–76. http://dx.doi.org/10.18063/IJB.2015.01.004.

1. Introduction

Polyetheretherketone (PEEK) is a semi-crystalline thermoplastic with excellent fibroblasts and osteoblasts biocompatibility, and with desirable mechanical properties such as strength, stiffness, and great thermal stability. Elastic modulus of PEEK is similar to that of cortical bone, which can reduce stress shielding following implantation. It is also radiolucent which permits radiographic assessment. The combination of these optimal properties has made PEEK of great potential for orthopaedic application. Medical grade PEEK-OPTIMA has been developed to meet the US Food and Drug Administration's (FDA) requirements and has been used in multiple clinical applications including spinal cage fusion and craniomaxillofacial reconstruction. Despite possessing favourable biomaterial properties as described above, PEEK is relatively bioinert, demonstrating poor osteointegration following implantation. Lack of biointegration can result in graft migration, and failure of the reconstructive procedure. Three main approaches are being developed to enhance bone apposition of PEEK-based implants for orthopaedic application:

- Incorporating bioactive materials such as calcium phosphates into PEEK to improve the bone-implant apposition,

- Coating PEEK implants with biomaterials such as titanium and/or calcium phosphates,
- Incorporating porosity into PEEK implants to enhance osteointegration and bone fixation.

Calcium phosphates including hydroxyapatite (HA) and β-tricalcium phosphate (β-TCP), or Bioglass can be utilised as composite filler to produce PEEK compounds with potential for osteointegration. Whilst addition of bioactive materials to PEEK offers an efficient method to engineer implants with tailored biomechanical properties, it may result in reduced strength and toughness of the implant[1]. Different processing methods such as compounding and injection moulding[2–4], compression moulding[5–8], cold press sintering[9–11] and selective laser sintering (SLS)[12–14] have been used to produce bioactive PEEK/HA and β-TCP composites.

Compounding and injection moulding is a low-cost process suitable for high-volume commercial near net shape manufacturing of PEEK compounds. However, the quantity at which bioactive fillers may be loaded is strictly limited, as high loading increases melt viscosity resulting in inconsistent and unreliable mixing[1]. Furthermore, material removal may be required to reveal bioactive particles on the surface of injection moulded PEEK compound. In cold press sintering, there is no limitation on the loading of bioactive fillers but the process suffers from residual porosity in composite due to pressure reduction during sintering. In contrast, compression moulding is a manufacturing platform offering greater flexibility, and shown to be well-suited to the synthesis of PEEK/HA composites. Compression moulding is low-cost, suitable for high-volume production of high-density PEEK compounds, and more critically tailored porosity. In this technique, porous PEEK compounds can be realized by the addition of a fugitive particle (e.g., sodium chloride) into the compound that is further leached out by soaking into a solvent post-moulding[1]. SLS, a powder-based additive manufacturing (AM) process, is capable of fabricating bioactive porous structures with very complex architecture, thus permitting greater design freedom. This process has been applied to form both porous natural grade PEEK and porous bioactive PEEK components. Use of SLS technique has been hampered by difficulty in loading the quantity of bioactive filler beyond 22% by volume (v/v), and exceeding porosity beyond 70%–74% (v/v)[13]. Compression moulding is perhaps the most appropriate form of material processing to produce bioactive PEEK compounds due to its ability to incorporate both porosity and bioactivity into PEEK with fewer limitations in terms of cost, pore interconnectivity, and level of bioactive filler loading in comparison to other techniques.

Current methods of bioactive PEEK processing, as discussed earlier, do not permit control on distribution of bioactive phase within the PEEK matrix. These techniques rely on simple mixing of PEEK with bioactive material powders/granules, and thus less control on distribution. In addition, the wide range of physical properties of different particles (size, shape, density) negates efficient and consistent mixing. The purpose of this study is to develop a novel technique that would permit greater control on incorporation of bioactive materials into PEEK than the existing techniques.

2. Materials and Methods

Figure 1 depicts workflow of the technique applied to make bioactive PEEK/HA composite. It comprises of fabrication of porous bioactive HA scaffold using extrusion-based AM technology, followed by PEEK melt infiltration into HA scaffolds through compression moulding process. To produce a fully interconnected porous PEEK, the produced PEEK/HA composite was further soaked into hydrochloric acid (HCl) solution so that the HA network could be removed by HCl etching. Solvent-based extrusion freeforming process, first developed by Evans and Yang's research group[15–25], was used to print highly uniform HA 3D lattice structures with controlled filament/pore size. In solvent-based extrusion freeforming, solidification is based on solvent evaporation which has advantages over similar techniques such as robocasting, where the state changes based on a dilatant transition.

The process of solvent-based extrusion freeforming of the HA scaffolds involved the following steps: (i) preparation of HA paste, (ii) 3D printing, and (iii) drying, debinding and sintering of the 3D printed scaffold. An extrusion-based 3D printer was designed and built in-house for 3D printing of porous HA scaffolds from HA paste.

The following materials were used to form the HA paste: (i) hydroxyapatite powder (HA, $Ca_{10}(PO_4)_6(OH)_2$, Grade P221 S, Plasma Biotal Ltd. UK) with density of 3156 $kg \cdot m^{-3}$ and particle size within the range of 1–5 μm (Figure 2(A)); (ii) polyvinyl butyral (PVB, Grade BN18, Whacker Chemicals, UK) with density of 1100 $kg \cdot m^{-3}$; (iii) polyethylene glycol (PEG, MW = 600, Whacker Chemicals, UK) with density of

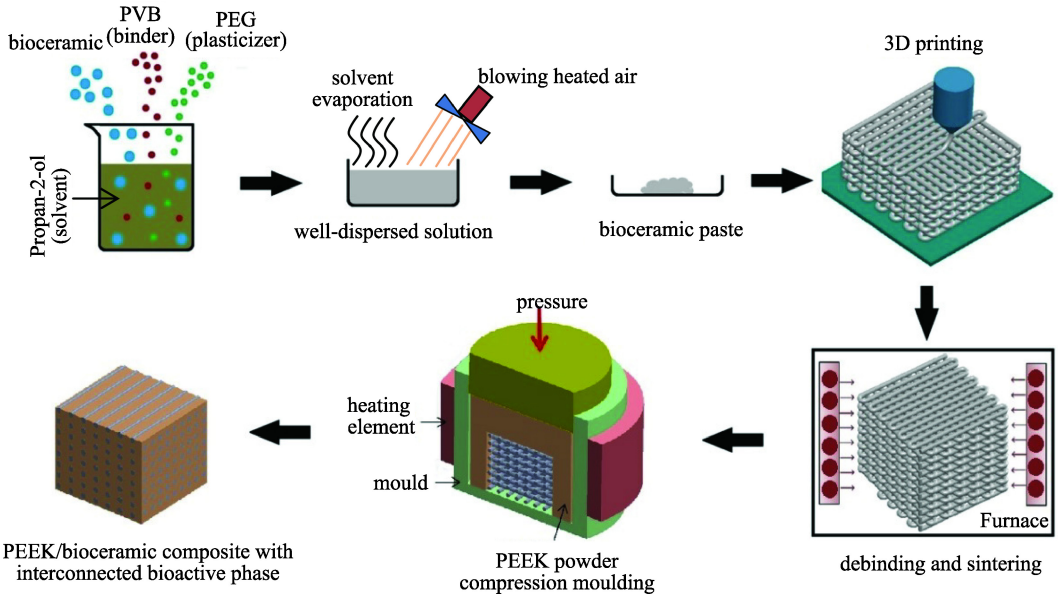

Figure 1. The workflow of the technique to integrate solvent-based extrusion freeforming and compression moulding for production of PEEK/HA composite.

1127 kg·m^{-3}; (iv) propan-2-ol (Fisher Scientific, UK) with density of 789 kg·m^{-3}. For production of HA paste, adhesive binder polyvinylbutyral (PVB), and plasticizer polyethyleneglycol (PEG) were fully dissolved in propan-2-ol solvent, with the ratio of 75% (w/v) PVB and 25% (w/v) PEG. HA powder was then added (60% (v/v) of HA based on the dried paste) to the solution, and stirred for 2 hours to achieve a well-dispersed solution. Following this, excess solvent was evaporated by fast stirring, and blowing hot air until a viscous HA paste was achieved. HA paste was then loaded into a homemade stainless steel syringe for 3D printing. Following the printing process, it is necessary to dry the scaffolds. Standard practice to achieve this is to leave the scaffold at room temperature for 24 hours to allow evaporation of excess solvent, and subsequently to place the scaffold in an oven for debinding and sintering. The sintering protocol of HA was developed from Evans and Yang' previous studies[22] in which the maximum sintering temperature was 1300℃ with a dwelling time of two hours.

The sintered HA scaffolds were overmoulded with PEEK OPTIMA®LT3 UF (Invibio Biomaterials Solutions, UK, used as received) through a compression moulding process using both static and dynamic loads to produce a PEEK/HA composite. PEEK OPTIMA®LT3 UF has a median particle size of 10 µm, (Figure 2(B)) and an average molecular weight of 83000 Da, which is an easy flow grade PEEK, with a melt index of 36.4 under conditions of 2.16 kg load in 10 min. The optimal temperature of 400℃ was determined through experimentation on overmoulding HA scaffolds with external dimensions of 10 × 10 × 3 mm, 250 µm filaments, and 200 µm pore sizes, with an optimal pressure of approximately 0.39 MPa. A mould with an internal diameter of 25 mm was prepared from tool steel, with appropriate ventilation on the inferior surface to avoid trapping air within the composite. Both static and dynamic loading methods were performed as follows:

• Static Loading: mould was heated up to 250℃, then load applied, and pressure maintained until the temperature reached 400℃. Temperature and load were maintained for a further 20 minutes (dwelling time), then heating was stopped, and the mould was left to cool under pressure, whereby the PEEK matrix crystallized and solidified. Composites were removed from the mould when the temperature had fallen to just below the glass transition temperature (143℃),

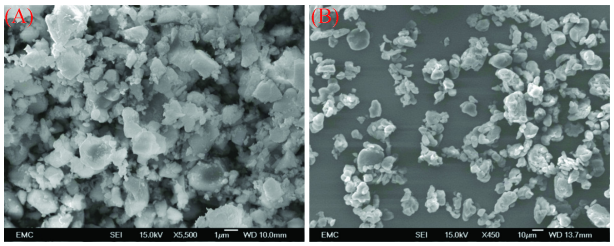

Figure 2. (A) Scanning electron micrograph of the used HA, (B) PEEK powder.

followed by cooling to room temperature, thus mitigating thermal stress and cracking.

• Dynamic Loading: Mould was heated up to 400℃ and maintained for 20 minutes. Load was applied for 5 seconds before heating was stopped, then the mould was left to cool under pressure, until the temperature fell below 143℃, at which the sample was removed.

A series of HA scaffolds with a range of filament and pore sizes were 3D printed, and subsequently overmoulded using dynamic loading to investigate the effects of filament/pore size on PEEK infiltration depth into the HA scaffold. The effect of dwelling time at the target temperature on the formation of PEEK HA composites was also explored. Through experimentation of the effect of load application during load and dwelling time, it was possible to optimize infiltration of molten PEEK through the HA pores without causing degradation of the polymer. Table 1 shows the details of the samples and the condition of the experiments. Samples were cut using diamond cutter (Mecatome T210, Presi, France). Infiltration depth was measured with the use of the optical microscopy (Olympus BH2-UMA, Japan). Scanning electron microscope (SEM) (JEOL JSM-6500F, Oxford Instruments, UK) was used for analysis of the samples. Static loading was also used to produce another set of PEEK/HA composites with a range of HA scaffold filament and pore sizes as shown in Table 2. Computed tomography (CT) (Custom 225 kV Nikon/Metris HMX ST) with a resolution of 9 µm per pixel (or 9 × 9 × 9 µm voxel) was performed to (i) determine HA percentage volume in the composite; (ii) investigate fractures in the HA network; and (iii) evaluate presence of air bubbles within the biocomposites after moulding. CT scanning of the composites was performed with a 225 kV X-ray source and Tungsten target and peak voltage was set to 120 kV with no pre-filtration. In order to achieve sufficient flux, 93 µA current was used (11.16 W). Throughout the 360 degrees rotation, 3142 projections were taken, with an average of 8 frames per projection to improve the signal to noise ratio. Exposure time of each projection was 177 ms with a gain of 30 dB. To reduce the effect of ring artefacts, shuttling was applied with a maximum displacement of 15 pixels. Projection data was reconstructed using Nikon's CTPro and CTAgent reconstruction software, which uses a filtered back projection algorithm. VG Studio Max 2.1 image processing application was used to standardize the volume (average volume of 220.14 mm^3) analysed from each sample.

3. Results

HA scaffolds with a range of filament and pore sizes were printed using the bespoke developed 3D printer. Through control of the printing parameters such as solvent content, paste deposition speed, and layer thickness, the microstructure of the scaffolds could be determined. HA filaments were delivered with high precision, with diameters down to 50 µm, achieved with the use of customized nozzle with a small die land length. The printed scaffolds were highly uniform, with a consistent and repeatable production process. Figures 3(A) and 3(B) depict SEM images of a sintered 3D printed HA scaffold, and a magnified image of a fractured region (the red rectangle),

Table 1. Specifications of the samples overmoulded under different conditions

HA scaffold size	Designed scaffold filament/pore size (µm)	Moulding pressure (MPa)	Loading type	Dwelling time (min)	Moulding temperature (℃)	Heating rate (℃/min)
10×10×3 mm	250/200	0.39	static	20	400	20
10×10×3 mm	400/400	0.39	dynamic	20	400	20
10×10×3 mm	400/500	0.39	dynamic	4, 12, 16, 20	400	20
10×10×3 mm	400/550	0.39	dynamic	20	400	20
10×10×3 mm	400/670	0.39	dynamic	20	400	20
20×18×3.7 mm	910/1200	0.39	dynamic	20	400	20

Table 2. Details of the PEEK/HA samples prepared for CT analysis; pressure 0.39 MPa, static loading, moulding temperature 400℃, dwelling time: 20 min, heating rate 20℃/min

Designed scaffold filament/pore size (µm)	250/200	250/400	400/250	400/400	400/550	400/700
Qt.	2	2	1	1	1	5

respectively. As seen in Figure 3(B), pores within the range of 1–5 µm in both fractured surface and external surfaces of the filament were realized through sintering. The rough surface of HA filaments has the potential to promote osteointegration *in vivo*. The main advantage of solvent-based extrusion freeforming is that both macroporosity of scaffold or spacing (yellow areas in Figure 3(A)) and microporosity of filaments (in Figure 3(B)) are controllable. Macroporosity was controlled via computer design, and microporosity via alternation in sintering temperature and dwelling time.

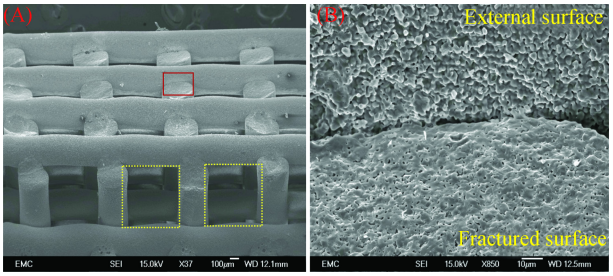

Figure 3. (A) A typical sintered HA scaffold with uniform microstructure and macroporosity (yellow rectangles), (B) a magnified image of the selected region (red rectangle) which includes both external and internal surface of filaments.

Like most conventional polymers, the viscosity of PEEK decreases with increasing temperature. The melting temperature of PEEK is approximately 340℃, and at temperatures of 360℃ to 400℃, the shear viscosity of PEEK varies from ~77×10^3 Pa·s to ~66×10^3 Pa·s. Therefore, to enable minimum shear viscosity, a mould temperature of 400℃ was used. Conrad *et al.*[26] demonstrated that this increased mould temperature may also increase the compressive modulus, yield strength and strain of the traditional PEEK/HA composites. Working temperatures greater than 380℃ have been shown to reduce crystallinity, which is known to be beneficial for ductility and toughness[27,28], with no adverse effect on biocompatibility *in vivo*[27]. Given the positive effects described on both shear viscosity and mechanical properties of the resulting PEEK samples, a mould temperature of 400℃ was selected for this study.

While mould temperatures of 400℃ guarantee minimum viscosity, caution must be exercised when working at temperatures in excess of 380℃ as there is a risk of thermal oxidation[26]. Potential of oxidation can be decreased by a reduction in dwelling time at the target temperature; as such optimisation of dwelling time is crucial. An insufficient dwelling time will result in inadequate melting of PEEK and therefore, failure to perfuse the scaffold pores at low pressure. Dwelling time must be sufficient to permit adequate heat transfer throughout the powder, including powder residing at a distance from the heat source. Conversely, prolonged time at the target temperature will result in thermal oxidation and degradation of the polymer. Samples with 400 µm filament and 500 µm pore sizes were overmoulded using dwelling times of 4, 12, 16, and 20 minutes, under dynamic loading (details in Table 1). Four minutes dwelling time was insufficient to melt the PEEK, 12 minutes resulted only in partial melting (Figure 4(A)), and 16 minutes dwelling time resulted in complete melting of the PEEK, but inadequate scaffold infiltration (Figure 4(B)). It was determined that 20 minutes was the optimal dwelling time for compression moulding of PEEK at 400℃, permitting adequate melt flowability to fill the lattice structures with no apparent polymer degradation. PEEK degradation was realized by visual observation (i.e., colour change in PEEK) in this study.

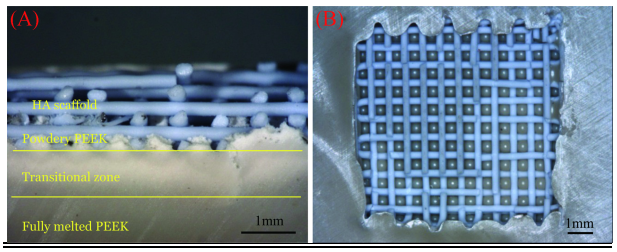

Figure 4. Bioactive PEEK/HA composites, scaffolds size 10 × 10 × 3 mm, filament size: 400 µm, pore size 500 µm, moulding temperature: 400ºC, pressure: 0.39 MPa, dynamic loading for 5 s; (A) dwelling time: 12 min, heating rate: 20℃/min, and (B) dwelling time: 16 min, heating rate: 20℃/min.

3D printed HA scaffolds are relatively fragile and moulding pressure must be carefully regulated to permit flow of molten PEEK and perfusion of fine pores without resulting in fracturing of the HA network. The results of our previous mechanical tests on extrusion freeformed HA scaffolds indicated that compressive loading must be less than 1 MPa[29], which is remarkably less than what has been reported for moulding of PEEK/HA powders. Roeder's group densified PEEK and HA-whisker dry powders at 125 MPa first, to avoid porosity, and then compression moulded at 250 MPa and 350℃–370℃[8]. Wong *et al.*[5] described an alternative technique in which PEEK and strontium-containing HA (Sr-HA) powders were densified at 35 MPa and then compression

moulded at 12–15 MPa and 350℃–375℃. The use of injection pressures of 11–14 MPa and temperature of 395℃was previously used in the injection moulding of PEEK/HA compounds[4]. Through experimentation, the optimal pressure to ensure full infiltration of a scaffold at size 10 × 10 × 3 mm without resulting in damage, was determined to be in the region of 0.39 MPa. The optimal pressure used in this study is similar to that used by other researchers in the compression moulding of reinforced carbon fibre-PEEK composites[30–32]. Luo *et al.*[30] tested pressures ranging from 0.5 to 2.0 MPa and found that 0.5 MPa is the most suitable pressure for making 3D carbon-fibre reinforced PEEK (CFR-PEEK) composites prepared by 3D co-braiding and compression moulding techniques. Mrse and Piggott[32] employed 0.4 MPa pressure for the preparation of AS-4 CFR-PEEK using lay-up followed by compression moulding process to avoid fibre damage. CT analysis was used to visualize the PEEK/HA composite and to detect overload-induced defects in HA network following compression moulding. Defects manifested in the form of either a partial crush, or micro-cracks (red arrows) in the HA filaments (Figure 5).

While the mechanical and biological functions of the composites can be tailored by varying the filament and pore size of the scaffold, there are lower limits for these parameters. Small filaments can fracture during compression moulding and molten PEEK is too viscous to infiltrate small pores. It was found that for scaffolds of 10 × 10 × 3 mm exposed to a moulding pressure of 0.39 MPa, the filament size and the spacing are required to be greater than 250 μm and 200 μm respectively to ensure successful PEEK infiltration without HA fracture. Dynamic compression was applied on PEEK/HA composites produced using scaffolds with a range of filament and pore sizes through conditions presented in Table 1. Infiltration depth was shown to be proportional to the pore size so that the scaffold, with dimensions of 20 × 18 × 3.7 mm, and filaments sized 910 μm while pores are 1200 μm, was found to be fully infiltrated by PEEK in both lateral and vertical directions, and HA network retained its structure and shape. For similar sized scaffolds that are 400 μm in filament size but of differing pore sizes (400, 500, 550 and 670 μm), the respective infiltration depths are as follows: 1.4, 1.9, 2.4 and 2.9 mm. When the infiltration depths—using dynamic loading—are compared with the infiltration as seen following static loading, it can be concluded even in scaffolds with pores of 200 μm that dynamic loading of the molten PEEK does not permit sufficient time for flow through the scaffold. Infiltration depth was found to be more dependent on the temporal application of pressure than the absolute magnitude of the pressure. Thus, different pore sizes ranging from 200 μm to 700 μm can be fully infiltrated easily using static loading without filament fracture. Furthermore, dynamic loading was found to result in greater entrapment of air in the PEEK/HA matrix than static loading. This implies that during dynamic loading, air is unable to escape from the PEEK matrix with a resulting decrease in mechanical strength.

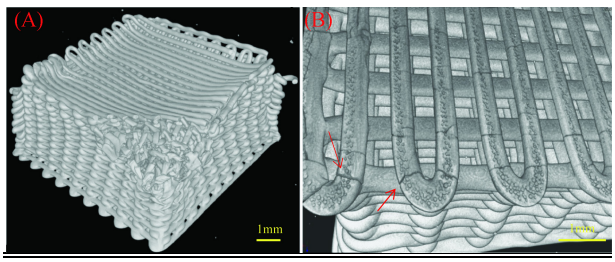

Figure 5. CT images of two typical damaged HA scaffolds after PEEK infiltration using excessive pressure; (A) partially crushed scaffold where filament is 250 μm and pore is 250 μm, (B) HA scaffold with micro-cracked filaments where filament is 400 μm and pore is 550 μm.

A static pressure of 0.39 MPa, dwelling time of 20 min and temperature of 400℃were found to be optimal for compression moulding of HA scaffolds of 10 × 10 × 3 mm in size with filament size above 250 μm and pore size above 200 μm. CT analysis of PEEK/HA composites where proportion of HA ranges from approximately 35% (v/v) to 77% (v/v) and are prepared by static loading, resulted in an average of 1.5% (v/v) air within the composite. CT scanning of the samples where scaffolds had larger pore size (i.e. less HA content) of 700 μm revealed that increasing pore size in the scaffolds can result in formation of more air bubble (up to approximately 7% (v/v)) within PEEK matrix. Figure 6 shows representative 3D images obtained using CT, imaging various cross sections of a typical PEEK/HA composite. The majority of air bubbles (which can be realized in dark color) are located superiorly in the images, which corresponds to the inferior surface of the mould where air release would be most likely to be impeded. The sintering-induced microporosity in HA filaments can be realized (the red arrow) in the magnified view in Figure 6(E).

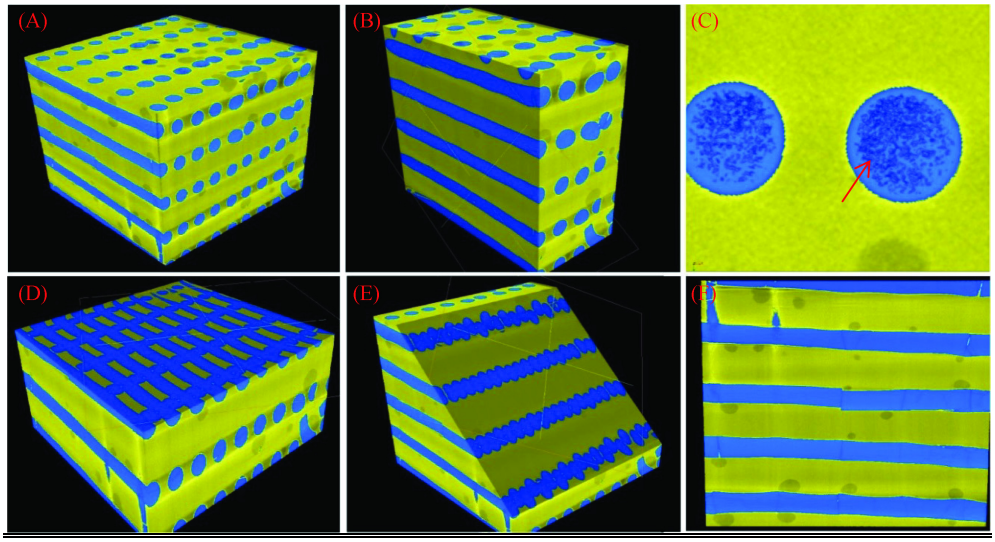

Figure 6. 3D image constructed from CT scan of a PEEK/HA composite with HA filament sized 400 µm and pore size of 700 µm; (A) isometric view (total volume 200.14 mm^3), (B) vertical section view, (C) horizontal section view, (D) oblique section view, (e) magnified view of HA filament within PEEK matrix, (F) front view of the PEEK/HA composite with broken/dislocated HA filaments.

Figures 7(A) and (B) depict SEM images of vertical sections from typical PEEK/HA composite produced successfully through compression moulding using static loading and PEEK-HA interface as seen in Figure 7(C)(the magnified view). Figure 7(D) shows a hole produced by soaking the PEEK/HA composite into HCl solution for 72 hours. HA filaments were dissolved in HCl, resulting in hollow channels suitable for cell attachment, infiltration and proliferation. As seen in Figures 7(A) and (B), HA scaffolds are fully infiltrated by PEEK in both vertical (infiltration depth was 3 mm) and lateral directions, while maintaining the HA network structure and uniformity. Whilst a good interface between HA filaments and PEEK matrix is realized (Figure 7(C)), this may not affect the mechanical properties of the composite. In CFR-PEEK, good bonding between PEEK matrix and carbon fibers is critical and determines the overall strength of the composite as it enables load transfer from PEEK to carbon fibers. However, in these PEEK/HA composites, the interface bonding might not be as important in CFR-PEEK since brittle HA filaments are used for its bioactivity, rather than its load-bearing properties. In contrast, HA scaffold volume fraction and filament diameter/layer orientation could be pivotal in determining the mechanical properties of the final composite, which is what we plan to investigate in the future. The interface achieved between HA filaments and PEEK matrix as shown in Figure 7(C) proves that the moulding temperature and pressure were appropriate selections.

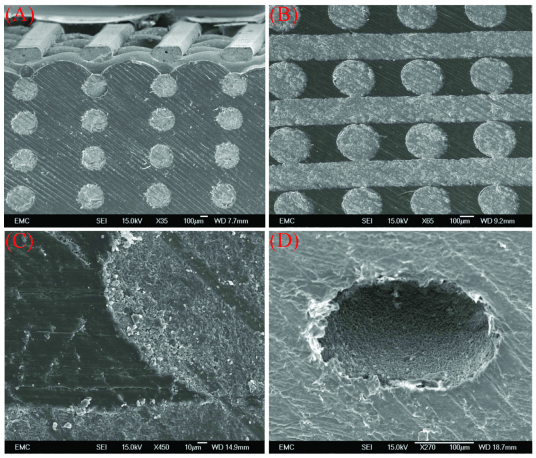

Figure 7. (A) and (B) Bioactive PEEK/HA composite: scaffold size 10 × 10 × 3 mm; HA scaffold filament size: 250 µm; moulding temperature: 400℃, dwelling time: 20 min, heating rate: 20℃/min, static pressure: 0.39 MPa; (C) close view of HA/PEEK interface; (D) a hole produced in PEEK by soaking PEEK/HA composite into HCl solution for 72 hours.

4. Discussion and Conclusion

Various manufacturing processes including the traditional chemical engineering methods and advanced AM techniques can be used for the construction of biomaterial scaffolds. Traditional techniques such as solvent casting/salt leaching, phase separation, foam-

ing, etc. have several limitations such as shape restrictions, manual intervention, inconsistency, and inflexibility. The use of solvent-based extrusion freeforming in this project guaranteed reproducibility and uniformity of the 3D printed HA scaffolds. Moreover, the technique can deliver much finer filaments (down to 50 μm) and avoid the thermal management issues of other extrusion-based techniques. The versatility of the method is not just in terms of structure and filament dimensions, but also in terms of the capability to utilize a range of ceramic powders (such as zirconia, alumina, HA, TCP, Bioglass, etc.) according to the desired properties. The key feature of our in-house developed solvent-based extrusion freeforming method is its unique nozzle design with minimum die land, and paste formulation, which allows us to make very uniform pastes quickly with an excellent extrudability and less nozzle jamming during extrusion. The additive nature of the process ensures minimal waste of biomaterial and renders it suitable for mass production of porous bioactive structures[33], and micro-scale woodpile structures[34] for use as scaffolds. The printed HA scaffolds were highly uniform which makes the overall process very consistent and repeatable for further use in compression moulding process.

A number of researchers have reported the use of polymer infiltration into bioceramic scaffolds to increase mechanical properties[35–40]. In these studies, bioceramic porous structures were immersed in molten polymer or solution to achieve infiltration of either the filaments or the entire structure. Martínez-Vázquez *et al.*[35] immersed extrusion freeformed β-TCP scaffolds into molten polylactic acid (PLA) and polycaprolactone (PCL) for 2 hours to produce composite bioceramic/polymer composite. These techniques were not suitable for use in this study as viscosity of easy flow medical grade PEEK is still much greater than PCL or PLA. This renders the process of infiltration of fine pores by immersion unreliable, resulting in scaffold material being retained on the surface of viscous PEEK melt. In addition, medical grade PEEK tends to degrade when it is held in excess of 30 minutes at temperatures above 400℃ in the absence of a vacuum. Ma *et al.*[41] used compression moulding to make a simple functionally graded PEEK/HA composites. Roeder's group at University of Notre Dame, USA, reported successful use of compression moulding and particulate leaching to make porous bioactive PEEK/HA-whisker composite[5–8]. Bioactive particles and/or a fugitive particle are mixed with PEEK powders, and then the mixture is densified by pressure, and finally, compression moulded. A similar compression moulding process was used in this study for infiltration of 3D printed HA lattice structures, barring the fact that there is no requirement for mixing and densification of PEEK and HA powders.

The proposed technique provides new possibilities for producing both bioactive PEEK compounds and porous PEEK structures with theoretically enhanced biological performance. In addition, both bioactive phase and PEEK matrix are fully interconnected, which is a superior advantage compared to existing techniques. Whilst HA, a well-known osteoconductive material was used in this work, other bioactive materials such as Bioglass, β-TCP, etc. with higher biodegradation rates can be used. The interconnected bioactive network can be fully absorbed *in vivo*, leaving 3D interconnected channels for further in-growth and proliferation. In this way, a 3D locked bone/PEEK structure could be achieved *in vivo* which can remarkably improve graft fixation compared with existing techniques.

In addition to PEEK/HA composite, the proposed technique could be utilized to produce PEEK with fully interconnected pores and controlled porosity. Conventional techniques such as particulate leaching exert poor control on porosity, and suffer from limitations such as inconsistency and require manual intervention. Using the proposed technique, porous PEEK could be easily produced with much greater control on porosity and enhanced reproducibility, a key requirement in production of medical devices. Furthermore, this technique is a low-cost process in comparison to SLS, while affording greater control of pore size (the minimum achievable in SLS is currently 400–500 μm). Therefore, while SLS as an AM technology has greater control on pore size and architecture of bioconstructs[42,43], its use in clinical applications is currently limited to those in which small pore sizes are not required. In contrast, with the use of the proposed technique, a wide range of pore sizes (200–1000 μm) is achievable. This makes the technique a versatile approach, enabling formation of porous PEEK which can be tailored to specific biomechanical requirements of a variety of clinical applications.

To summarize, the main features of these new PEEK/HA composite are:

• Greater control on distribution of bioactive phase within PEEK matrix (controlled by computer design),

• Ability to tailor mechanical and biological proper-

ties by varying percentage of bioactive phase (by either varying HA filament or pore size),

• Various bioactive materials such as Bioglass, β-TCP, etc. with faster biodegradation rate than HA can be served so that the bioactive network leaves 3D interconnected channels after absorbing *in vivo* for further bone cells in-growth and proliferation,

• 100% interconnectivity of both bioactive network and PEEK brings about maximum structural integrity of the composite,

• Ability to incorporate bioactive materials with a very high volumetric percentage (in this study up to 77% (v/v) HA) for non-load bearing applications such as craniomaxillofacial plates, etc.

Quality control standards stipulate that testing of medical device biocompatibility requires extensive investigation in order to confirm the true readiness for clinical application. As a precursor to future developments, our objective for this study was to show the preliminary evidences supporting feasibility of compression moulding of very fragile HA scaffolds with PEEK. Further studies have been planned to include mechanical properties assessment, and *in vitro* cell differentiation, proliferation and molecular assays.

Conflict of Interest

No conflict of interest was reported by the authors.

Acknowledgments

The authors are grateful to Invibio Biomaterial Solutions Ltd., and the Faculty of Engineering and the Environments, University of Southampton for their financial support. The authors acknowledge the μ-VIS centre at the University of Southampton, and Dr. Orestis L. Katsamenis for provision of tomographic imaging facilities, supported by EPSRC grant EP-H01506X.

References

1. Roeder R K and Conrad T L, 2012, Bioactive polyaryletherketone composites, in *PEEK Biomaterials Handbook.* William Andrew Publishing, Oxford, 163–179.
2. Abu Bakar M S, Cheng M H W, Tang S M, *et al.* 2003, Tensile properties, tension–tension fatigue and biological response of polyetheretherketone–hydroxyapatite composites for load-bearing orthopedic implants. *Biomaterials,* vol.24(13): 2245–2250. http://dx.doi.org/10.1016/S0142-9612(03)00028-0.
3. Tang S M, Cheang P, AbuBakar M S, *et al.* 2004, Tension–tension fatigue behavior of hydroxyapatite reinforced polyetheretherketone composites. *International Journal of Fatigue,* vol.26(1): 49–57. http://dx.doi.org/10.1016/S0142-1123(03)00080-X.
4. Abu Bakar M S, Cheang P and Khor K A, 2003, Mechanical properties of injection molded hydroxyapatite–polyetheretherketone biocomposites. *Composites Science and Technology,* vol.63(3–4): 421–425. http://dx.doi.org/10.1016/S0266-3538(02)00230-0.
5. Wong K L, Wong C T, Liu W C, *et al.* 2009, Mechanical properties and *in vitro* response of strontium containing hydroxyapatite/polyetheretherketone composites. *Biomaterials,* vol.30(23–24): 3810–3817. http://dx.doi.org/10.1016/j.biomaterials.2009.04.016.
6. Converse G L, Yue W and Roeder R K, 2007, Processing and tensile properties of hydroxyapatite-whisker-reinforced polyetheretherketone. *Biomaterials,* vol.28(6): 927–935. http://dx.doi.org/10.1016/j.biomaterials.2006.10.031.
7. Converse G L, Conrad T L and Roeder R K, 2009, Mechanical properties of hydroxyapatite whisker reinforced polyetherketoneketone composite scaffolds. *Journal of the Mechanical Behavior of Biomedical Materials,* vol.2(6): 627–635. http://dx.doi.org/10.1016/j.jmbbm.2009.07.002.
8. Converse G L, Conrad T L, Merrill C H, *et al.* 2010, Hydroxyapatite whisker-reinforced polyetherketoneketone bone ingrowth scaffolds. *Acta Biomaterialia,* vol.6(3): 856–863. http://dx.doi.org/10.1016/j.actbio.2009.08.004.
9. Yu S C, Hariram K P, Kumar R, *et al.* 2005, *In vitro* apatite formation and its growth kinetics on hydroxyapatite/polyetheretherketone biocomposites. *Biomaterials,* vol.26(15): 2343–2352. http://dx.doi.org/10.1016/j.biomaterials.2004.07.028.
10. Hengky C, Kelsen B, Saraswati, *et al.* 2009, Mechanical and biological characterization of pressureless sintered hydroxapatite-polyetheretherketone biocomposite. *IFMBE Proceedings—13th International Conference on Biomedical Engineering,* vol.23: 261–264. http://dx.doi.org/10.1007/978-3-540-92841-6_63.
11. Kim I Y, Sugino A, Kikuta K, *et al.* 2009, Bioactive composites consisting of PEEK and calcium silicate powders. *Journal of Biomaterials Applications,* vol. 24(2): 105–118. http://dx.doi.org/10.1177/0885328208094557.
12. Tan K H, Chua C K, Leong K F, *et al.* 2003, Scaffold development using selective laser sintering of polyetheretherketone–hydroxyapatite biocomposite blends. *Biomaterials,* vol.24(18): 3115–3123. http://dx.doi.org/10.1016/S0142-9612(03)00131-5.

13. Tan K H, Chua C K, Leong K F, *et al.* 2005, Fabrication and characterization of three-dimensional poly(ether-ether-ketone)/-hydroxyapatite biocomposite scaffolds using laser sintering. *Proceedings of the Institution of Mechanical Engineers, Part H: Journal of Engineering in Medicine,* vol.219(3): 183–194. http://dx.doi.org/10.1243/095441105x9345.
14. Schmidt M, Pohle D and Rechtenwald T, 2007, Selective laser sintering of PEEK. *CIRP Annals-Manufacturing Technology*, vol.56(1): 205–208. http://dx.doi.org/10.1016/j.cirp.2007.05.097.
15. Yang S, Yang H, Chi X, *et al.* 2008. Rapid prototyping of ceramic lattices for hard tissue scaffolds. *Materials & Design,* vol.29(9): 1802–1809. http://dx.doi.org/10.1016/j.matdes.2008.03.024.
16. Lu X S, Lee Y J, Yang S F, *et al*. 2009, Fabrication of millimeter-wave electromagnetic bandgap crystals using microwave dielectric powders. *Journal of the American Ceramic Society,* vol.92(2): 371–378. http://dx.doi.org/10.1111/j.1551-2916.2008.02907.x.
17. Lu X S, Lee Y J, Yang S F, *et al.* 2010, Solvent-based paste extrusion solid freeforming. *Journal of the European Ceramic Society,* vol.30(1): 1–10. http://dx.doi.org/10.1016/j.jeurceramsoc.2009.07.019.
18. Lu X S, Lee Y J, Yang S F, *et al.* 2009, Extrusion freeforming of millimeter-wave electromagnetic band-gap (EBG) photonic crystals. *Tsinghua Science and Technology,* vol.14(S1): 168–174. http://dx.doi.org/10.1016/S1007-0214(09)70087-2.
19. Lu X S, Lee Y J, Yang S F, *et al.* 2009, Fine lattice structures fabricated by extrusion freeforming: Process variables. *Journal of Materials Processing Technology,* vol.209(10): 4654–4661. http://dx.doi.org/10.1016/j.jmatprotec.2008.11.039.
20. Lu X S, Lee Y J, Yang S F, *et al*. 2009. Extrusion freeforming of millimeter wave electromagnetic band-gap (EBG) structures. *Rapid Prototyping Journal*, vol. 15(1): 42–51. http://dx.doi.org/10.1108/13552540910925054.
21. Lu X S, Lee Y J, Yang S F, *et al.* 2008, Fabrication of electromagnetic crystals by extrusion freeforming. *Metamaterials,* vol.2(1): 36–44. http://dx.doi.org/10.1016/j.metmat.2007.12.001.
22. Yang H Y, Yang S F, Chi X P, *et al.* 2008, Sintering behaviour of calcium phosphate filaments for use as hard tissue scaffolds. *Journal of the European Ceramic Society,* vol.28(1): 159–167. http://dx.doi.org/10.1016/j.jeurceramsoc.2007.04.013.
23. Lu X S, Chen L F, Amini N, *et al.* 2012, Novel methods to fabricate macroporous 3D carbon scaffolds and ordered surface mesopores on carbon filaments. *Journal of Porous Materials,* vol.19(5): 529–536. http://dx.doi.org/10.1007/s10934-011-9501-x.
24. Yang H, Yang S, Chi X, *et al.* 2006, Fine ceramic lattices prepared by extrusion freeforming. *Journal of Biomedical Materials Research Part B: Applied Biomaterials,* vol.79B(1): 116–121. http://dx.doi.org/10.1002/jbm.b.30520.
25. Yang H Y, Thompson I, Yang S F, *et al.* 2008, Dissolution characteristics of extrusion freeformed hydroxyapatite–tricalcium phosphate scaffolds. *Journal of Materials Science: Materials in Medicine,* vol.19(11): 3345–3353. http://dx.doi.org/10.1007/s10856-008-3473-7.
26. Jaekel D J, Macdonald D W and Kurtz S M, 2011, Characterization of PEEK biomaterials using the small punch test. *Journal of the Mechanical Behavior of Biomedical Materials,* vol.4(7): 1275–1282. http://dx.doi.org/10.1016/j.jmbbm.2011.04.014.
27. Nieminen T, Kallela I, Wuolijoki E, *et al.* 2008, Amorphous and crystalline polyetheretherketone: mechanical properties and tissue reactions during a 3-year follow-up. *Journal of Biomedical Materials Research Part A,* vol.84A(2): 377–383. http://dx.doi.org/10.1002/jbm.a.31310.
28. Conrad T L, Jaekel D J, Kurtz S M, *et al.* 2013, Effects of the mold temperature on the mechanical properties and crystallinity of hydroxyapatite whisker-reinforced polyetheretherketone scaffolds. *Journal of Biomedical Materials Research Part B: Applied Biomaterials,* vol.101B(4): 576–583. http://dx.doi.org/10.1002/jbm.b.32859.
29. Yang H Y, Chi X P, Yang S, *et al.* 2010, Mechanical strength of extrusion freeformed calcium phosphate filaments. *Journal of Materials Science: Materials in Medicine,* vol.21(5): 1503–1510. http://dx.doi.org/10.1007/s10856-010-4009-5.
30. Luo H L, Xiong G Y, Yang Z W, *et al.* 2014, Preparation of three-dimensional braided carbon fiber-reinforced PEEK composites for potential load-bearing bone fixations. Part I. Mechanical properties and cytocompatibility. *Journal of the Mechanical Behavior of Biomedical Materials,* vol.29: 103–113. http://dx.doi.org/10.1016/j.jmbbm.2013.09.003.
31. Tai N H, Ma C C M and Wu S H, 1995, Fatigue behaviour of carbon fibre/PEEK laminate composites. *Composites,* vol.26(8): 551–559. http://dx.doi.org/10.1016/0010-4361(95)92620-R.
32. Mrse A M and Piggott M R, 1993, Compressive properties of unidirectional carbon fibre laminates: The effects of unintentional and intentional fibre misalignments. *Composites Science and Technology,* vol.46(3): 219–227.

http://dx.doi.org/10.1016/0266-3538(93)90156-B.

33. Vaezi M, Chianrabutra S, Mellor B, et al. 2013, Multiple material additive manufacturing – Part 1: a review. *Virtual and Physical Prototyping,* vol.8(1): 19–50. http://dx.doi.org/10.1080/17452759.2013.778175.
34. Vaezi M, Seitz H and Yang S F, 2013, A review on 3D micro-additive manufacturing technologies. *The International Journal of Advanced Manufacturing Technology,* vol.67(5–8): 1721–1754. http://dx.doi.org/10.1007/s00170-012-4605-2.
35. Martínez-Vázquez F J, Perera F H, Miranda P, *et al.* 2010, Improving the compressive strength of bioceramic robocast scaffolds by polymer infiltration. *Acta Biomaterialia,* vol.6(11): 4361–4368. http://dx.doi.org/10.1016/j.actbio.2010.05.024.
36. Seol Y J, Park D Y, Park J Y, *et al.* 2013, A new method of fabricating robust freeform 3D ceramic scaffolds for bone tissue regeneration. *Biotechnology and Bioengineering,* vol.110(5): 1444–1455. http://dx.doi.org/10.1002/bit.24794.
37. Lee B T, Quang D V, Youn M H, *et al.* 2008, Fabrication of biphasic calcium phosphates/polycaprolactone composites by melt infiltration process. *Journal of Materials Science: Materials in Medicine,* vol.19(5): 2223–2229. http://dx.doi.org/10.1007/s10856-007-3279-z.
38. Fedotov A Y, Bakunova N V, Komlev V S, *et al.* 2013, Increase in mechanical properties of porous materials by polymer impregnation. *Inorganic Materials: Applied Research,* vol.4(1): 7–11. http://dx.doi.org/10.1134/S2075113313010048.
39. Alge D L and Chu T M G, 2010, Calcium phosphate cement reinforcement by polymer infiltration and *in situ* curing: a method for 3D scaffold reinforcement. *Journal of Biomedical Materials Research Part A,* vol.94A(2): 547–555. http://dx.doi.org/10.1002/jbm.a.32742.
40. Bang L T, Kawachi G, Nakagawa M, *et al*. 2013, The use of poly (ε-caprolactone) to enhance the mechanical strength of porous Si-substituted carbonate apatite. *Journal of Applied Polymer Science,* vol.130(1): 426–433. http://dx.doi.org/10.1002/app.39164.
41. Ma R, Fang L, Luo Z K, *et al.* 2014, Mechanical performance and *in vivo* bioactivity of functionally graded PEEK–HA biocomposite materials. *Journal of Sol-Gel Science and Technology,* vol.70(3): 339–345. http://dx.doi.org/10.1007/s10971-014-3287-7.
42. Duan B, Cheung W L and Wang M, 2011, Optimized fabrication of Ca-P/PHBV nanocomposite scaffolds via selective laser sintering for bone tissue engineering. *Biofabrication*, vol.3(1): 015001. http://dx.doi.org/10.1088/1758-5082/3/1/015001.
43. Huang W, Feng P, Gao C D, *et al.* 2015, Microstructure, mechanical, and biological properties of porous poly(vinylidene fluoride) scaffolds fabricated by selective laser sintering. *International Journal of Polymer Science*, vol.2015: 1–9. http://dx.doi.org/10.1155/2015/132965.